Desalination and Water Treatment
www.deswater.com

doi:10.5004/dwt.2017.20190

66 (2017) 274–280
March

Effect of heat treatment on the surface properties of selected bituminous shale for cationic dye sorption

Asmae Gouza, Kenza Fanidi, Sanaa Saoiabi, Abdelaziz Laghzizil, Ahmed Saoiabi

Laboratoire de Chimie Physique Générale, Faculté des Sciences, Université Mohammed V, Av. Ibn batouta BP.1014 Agdal Rabat, Morocco, email: asmae_gouza@yahoo.fr (A. Gouza), kenza_fanidi@live.fr (K. Fanidi), sanaa.saoiabi@yahoo.com (S. Saoiabi), laghzizi@fsr.ac.ma (A. Laghzizil), saoiabi_ahmed@yahoo.fr (A. Saoiabi)

Received 16 May 2016; Accepted 18 August 2016

ABSTRACT

Due to increasing contamination of water and soils by industrial production, there is a crucial need for new natural sorbents that are cost-effective, environmental friendly for pollutant removal. In this context, Moroccan oil shale from Tangier Region (OST) was characterized and evaluated for methylene blue (MB) remediation as model for cationic dye. The maximal sorption capacity of the dried OST100 (>100 mg g^{-1}) is higher than that of calcined OST550 (80 mg g^{-1}) and OST950 (60 mg g^{-1}) samples. The pseudo-second-order kinetic model and Freundlich equation were found the most adequate to reproduce the experimental data. The effect of the thermal treatment of this oil shale on its sorption capacity was investigated, demonstrating that the active sites from shale play an important role for MB removal. As a result, this natural, widely available and low-cost resource can be a good adsorbent used for many removal applications of specific pollutants.

Keywords: Oil shale; Thermal treatment; Valorization; Surface properties; Dye adsorption

1. Introduction

Water pollution by toxic chemical species may pose a serious threat to humans and environment. Dyes are among the major organic compounds encountered in wastewaters, which are considered dangerous and harmful to living systems. Consequently, many treatment processes have been applied to reduce dye concentration from wastewaters. Adsorption is considered an effective method that was extensively used in the last few years using natural and synthetic adsorbents such as activated carbon, fly ash [1], clay minerals and soil [2], quartz, calcite, kaolinite and α-alumina [3], Mg-Al-layered double hydroxides [4], sepiolite clay kerolites [5], resins [6], and natural phosphate [7]. The choice of the suitable adsorbent depends on its adsorption capacity, availability and cost. The utilization of natural adsorbents with a high adsorption activity is an interesting alternative to (i) eliminate their harmful effect on the environment and (ii) provide a profitable use of these materials. Recently, it was shown that the oil shale is a promising and efficient low cost adsorbent for organic and inorganic pollutants [8–11]. However, the chemical composition of these rocks varies from one deposit to another. Oil shale can be classified by their chemical composition or by their depositional environment. Therefore, bituminous shale from Tangier (Morocco) was selected for the treatment of wastewater as a potential alternative to the conventional treatment versus cationic dye. We selected the methylene blue dye as model for cationic dyes, related to its large application for coloring different industrial materials; there is a constant interest in removing it from aqueous solutions by using the raw and the thermally treated oil shale as a widely available and low-cost resource in Morocco. Noticeably, no detailed information on the sorption properties of studied oil shale is available so far. Therefore, its capacity for the removal of the methylene blue as a model for cationic dye was investigated and compared to the performance of its thermal treatments.

---

*Corresponding author.

2. Materials and methods

2.1. Sedimentary schist rock

The bituminous shale used in this study comes from Tangier layers located in the north of Morocco, nearby to the street of Gibraltar, the sea narrowness, which connects the Mediterranean Sea with the Atlantic. Prior use of this material requires initial treatments such as crushing and washing. The fraction of 100–500 µm grain size was washed with distilled water for several times to remove the soluble matter. This naturally oil shale is composed from the organic matter chemically linked to the mineral species. The main chemical composition was determined as follows: 80%SiO_2, 7.9%Al_2O_3, 2.17%Fe_2O_3, 1.21%MgO, 0.84%CaO, 0.64%K_2O, 0.31%Na_2O, 0.2%TiO_2, 0.14%ZnO, and 0.1% SO_3 [12]. The structure and morphology of this schist was estimated using different characterization techniques. Thermogravimetric analysis showed that the quantity of the organic component is about 8 wt.%, and it is lower than other Moroccan oil shale (20 wt.%) [13,14]. It should notice that the heating rate has a little effect on the variation of the mass losses and the combustion temperature.

The crystalline structure of oil shale from Tangier (Morocco) (namely OST100) was examined by x-ray diffraction at different temperatures of calcination. The high intensity of XRD peaks indicates that OST100 powder has a high crystallinity. Therefore, x-ray patterns of this raw material shows a main phase attributed to the SiO_2-quartz associated with minor oxide phases such as calcite, Fe_2O_3 and Al_2O_3 (Fig. 1).

By heating OST100 sample at a temperature up to 550°C (OST550) and 950°C (OST950), some reflections disappeared due to the transformation of hydroxyls (OH species) into oxide groups, decarbonation of calcite and decomposition of some organic matter present in the raw OST powder such as provide by TG analysis. As consequence, no significant evolution of the crystalline structure of the mineral phases upon heating has observed. Using solid state ^{29}Si-NMR with different CP-MAS contact time (Fig. 2), a main resonance of SiO_2-quatz at –107 ppm is detected in OST100, but a second broad pick found at –97 ppm particularly for less CP-MAS contact time attributed to amorphous silica.

Taken together, these data indicate that the raw OST100 material contains only silica quartz unconnected to other mineral species. The result is also confirmed by the infrared spectroscopy. The vibration bands at 1170 cm^{-1}, 1010 cm^{-1}, 695 cm^{-1} and 675 cm^{-1} are attributable to SiO_2 absorption vibrations. In the addiction, two bands at 1382 cm^{-1} and 868 cm^{-1} indicate the presence of carbonate groups in raw material OST100. The minor bands due to the presence of organic carbon appear through the bands at 3380, 2280, 2170, 1969 cm^{-1}.

The measure of the specific surface of the OST samples was realized by multi-points N_2-sorption isotherms. In the case of OST100 and OST550, their isotherms correspond to mesoporous materials, while OST950 presents micropores. Further, the surface area of dried OST100 (27 m^2 g^{-1}) is much higher than that of OST550 (23 m^2 g^{-1}) and OST950 (3.5 m^2 g^{-1}) related to the granular growth that reduced the surface pores such as reported in several works [7,12,15]. This is confirmed by calculation of the pore size distribution using the BJH model indicating a large distribution toward 3.7 nm for OST100 and OST550 that slightly narrows down to 20 nm for OST950.

2.2. Sorption experiments

Adsorption kinetics were followed in batch experiments conducted at 25°C by adding 200 mg of sorbent to 100 mL of an aqueous solution containing 20 mg L^{-1} of MB dye at natural pH 5.6. Sorption isotherm studies were conducted in varying the initial concentration from 5 to 500 mg L^{-1}. At the selected time interval, the suspensions were sampled through centrifuged. The dye concentration in the supernatant was monitored using a UV-visible spectrophotometer (Perking Elmer Lamda II) at λ = 662 nm. All UV-visible analyses were controlled by high performance liquid chromatography (HPLC). The amount of sorbed dye was calculated by using the equation:

$$q_t = (C_0 - C_t) \cdot V/m \tag{1}$$

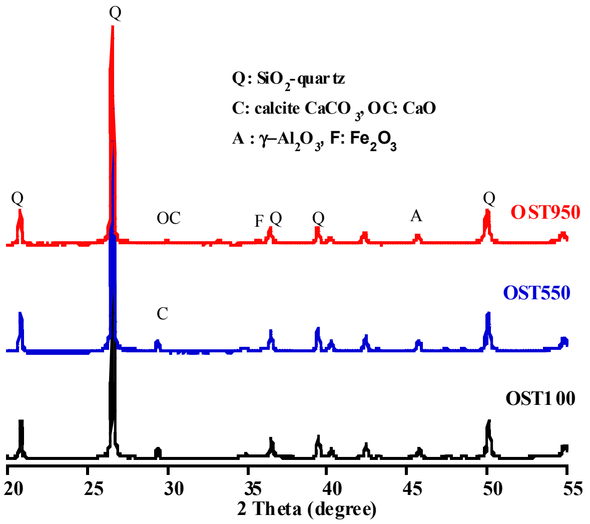

Fig. 1. X-ray patterns of OST samples at various temperature of calcination.

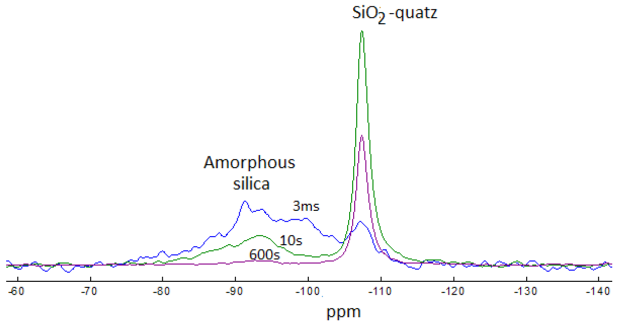

Fig. 2. ^{29}Si-NMR spectra of natural oil shale OST100 from Tangier-Morocco with CP-MAS contact time.

where q_t (mg g^{-1}) is the amount of the adsorbed dye at time t, C_0 and C_t are the dye concentration in solution (mg L^{-1}) at $t = 0$ and $t = t$, V is the volume (L) of dye solution and m is the weight (g) of the sorbent. All experiments were carried out in triplicate. The mean values are reported and the error range was inferior to 5%.

In order to determine the kinetics parameters of the sorption reactions, Lagergren pseudo-first order and pseudo-second order models have been applied to the experimental data. The Lagergren pseudo-first order equation can be expressed as [16]:

$$\log (q_e - q_t) = \log q_{e,1} - (k_1/2.303) \cdot t \tag{2}$$

where q_e and $q_{e,1}$ are the experimental and calculated amount of adsorbed dye at equilibrium(mg g^{-1}) and k_1 the first order kinetic constant (min^{-1}).This model can be applied if log $(q_e - q_t)$ vs. t gives a straight line.

The pseudo-second order model can be expressed as a differential equation [17]:

$$t/q_t = 1/k_2 q^2_{e,2}) + (1/q_{e,2}) \cdot t \tag{3}$$

where $q_{e,2}$ is the calculated amount of adsorbed dye at equilibrium(mg g^{-1}) and k_2 the second order kinetic constant (g mg^{-1} min^{-1}). The plot of t/q_t against time t of Eq. (3) should give a linear relationship.

Sorption isotherms were analyzed using the Langmuir and Freundlich models. The Langmuir equation can be written as:

$$C_e/q_e = 1/\beta . q_{e,L} + C_e/q_{e,L} \tag{4}$$

where $q_{e,L}$ is the calculated maximum amount of adsorbed dye at equilibrium(mg g^{-1}), and β is the Langmuir constant (L · mg^{-1}) related to the adsorption energy $q_{e,L}$ and β can be obtained by plotting C_e/q_e vs. C_e. The Freundlich model can be written as :

$$q_e = K_f C_e^{1/n} \tag{5}$$

where K_f is an approximate indicator of adsorption capacity, while $1/n$ is a function of the strength of adsorption in the adsorption process. A linear form of this model is :

$$\log q_e = \log K_f + 1/n \log C_e.$$

3. Results and discussions

In a first step, the effect of contact time on the methylene blue (MB) dye adsorption was studied for an initial concentration of 20 mg L^{-1} and an adsorbent dose of 2 g L^{-1} at room temperature and an initial pH 5.6. Kinetics investigations were carried out to measure the rate of reaction under various experimental conditions and to determine the time required to reach equilibrium of the sorption process. The resulting data suggest that MB dye is quickly adsorbed onto OST surfaces within the first minutes (Fig. 3).

The thermal treatment of the oil shale had an impact on the sorption capacity of MB but not significantly greatly on kinetic reaction. With 20 ppm of MB dye, the maximal adsorbed amounts on OST100 (9.5 mg · g^{-1}) and calcined OST550 (7.7 mg · g^{-1}) are more important for that of OST950 (3.9 mg · g^{-1}). Therefore, the removal of MB by OST100 is almost totally reached for OST100 (95%) but less for OST550 (77%). Therefore, OST100 can be considered as adsorbent and could be effective for the treatment of MB dye-rich wastewater. To determine the kinetic parameters, the pseudo-first order and the pseudo-second-order kinetics models were evaluated to simulate the sorption data. Kinetics parameters are given in Table 1. The pseudo-second order model was the suitable model for the MB dye sorption independently of the thermal treatment of the sorbents. The kinetics constants vary in the order k_2(OST100) > k_2(OST550) > k_2(OST950).

Based on previous kinetics data, sorption isotherms were obtained after 3 h as contact time, showing that OST100 exhibits a higher dye sorption capacity than OST550 and OST950. The influence of adsorbent dose on MB sorption was also studied (Fig. 4). It was found that with the increasing dosage of adsorbent the MB removal from water is favoured and the optimal dose is required with 2 g L^{-1}. Insignificant change was observed when the adsorbent dose was increased up 2 g L^{-1}, suggesting that after this dose, the saturation of active site was attained and the adsorption of MB molecules onto OST surface is limited. The thermal treatment of the powders did not significantly modify these trends. On this basis, a 2 g L^{-1} dose of the OST adsorbent was selected for the rest of our study.

The retention capacity of raw oil shale OST100 and the heat-treated OST550 and OST950 powders, was then studied by performing sorption isotherms for initial dye concentrations ranging from 5 mg L^{-1} to 500 mg L^{-1} over 3 h (Fig. 5). The amount of adsorbed dye increases with its initial concentration in the MB contaminated solution. Higher capacity was obtained with OST100 (> 100 mg g^{-1}). Considering the effect of the thermal treatment of OST sorbent, the first heating step from 100°C to 550°C do not significantly affect the mineral surface nor the powder porous structure. Therefore, the little decrease in sorption capacity can be attributed to the removal of the organic matter at 550°C (5 wt% as weight loss). Heating further to 950°C

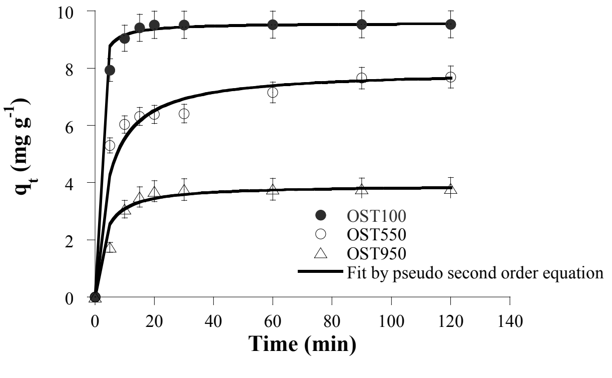

Fig. 3. Evolution of the amount of sorbed dye (q_t) with contact time "t" on the dried OST and calcined OST powder. Plain lines (–) correspond to the simulation of experimental data with the pseudo-second order model. (C_0 = 20 mg L^{-1}, dose = 2 g/L, T = 25°C, pH = 5.6).

Table 1
Kinetic rate constants (k_i) and adsorption capacities ($q_{e,i}$) obtained by using pseudo-first order and pseudo-second order models to MB molecules adsorbed on the oil shale. R^2 indicate the correlation coefficients for the linear fits

	Pseudo first order model			Pseudo second order model		
	k_1 (min^{-1})	$q_{e,1}$ (mg g^{-1})	R^2	k_2 (g mg^{-1}min^{-1})	$q_{e,2}$ (mg g^{-1})	R^2
OST100	0.187	1.79	0.9017	0.224	9.57	0.9999
OST550	0.022	2.25	0.8407	0.030	7.91	0.9992
OST950	0.160	3.71	0.8901	0.019	3.89	0.9993

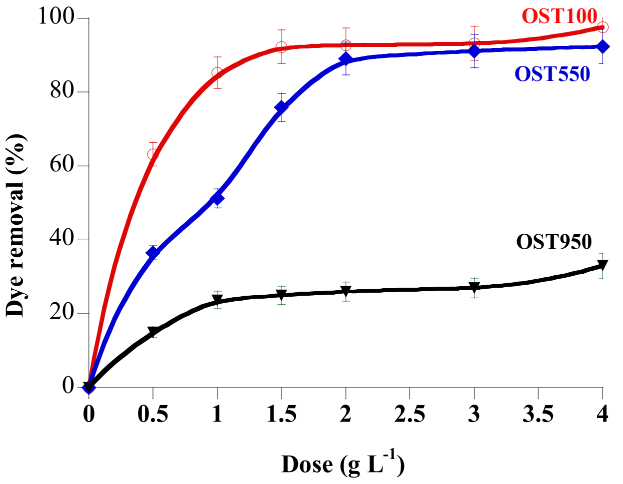

Fig. 4. Effect of adsorbent dose on the removal of MB dye using dried and treated oil shale. (C_0 = 20 mg L^{-1}, t = 3 h, T = 25°C, pH = 5.6).

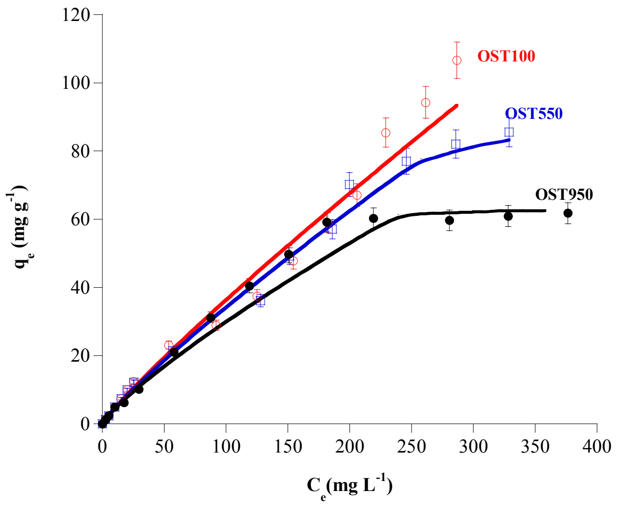

Fig. 5. Variation of sorbed MB content (q_e) with MB concentration with the OST powders. Plain lines (–) correspond to the curves obtained by fitting the data with the Freundlich equation. Dose = 2 g L^{-1}, contact time = 3 h, temperature = 25°C, pH = 5.6).

sample, the specific surface area is reduced and the OST950 surface became more hydrophobic due to silanol condensation [18–20], resulting in moderate decrease in kinetics rate and maximum sorption capacity. The sorbent saturation was reached for OST550 and OST950 and their experimental maximum capacities q_{max} are 60 mg g^{-1} and 80 mg g^{-1}, respectively, however, the sorption isotherms did not reach a plateau for OST100 related to the higher affinity towards MB molecules (q_{max} > 100 mg g^{-1}).

Attempts to use the Langmuir model were unsuccessful, while the Freundlich equation is correct fitting of the experimental data, which supposes some types of interactions between adsorbing molecules. Such interactions can be ascribed to the forces among cationic dye molecule into the OST sorbent interfacial space. The parameters extracted from these analyses are gathered in Table 2. The most reliable fits (i.e. larger R^2 values) were obtained with the Freundlich model. To analyze these data, it is first important to consider the relative charge of the sorbents and MB dye. The isoelectric point (IEP) of quartz was reported to vary between 1.5 and 3, so it is negatively-charged in the conditions of these experiments [21] while the MB dye was charged positively at acid pH. Thus, the possible mechanism involving MB sorption with shale should be associated to the surface complexation reactions. To get additional information on the adsorption mechanism, the pH evolution of the MB solution was also monitored during the sorption process (Fig. 6).

When the adsorbents are dispersed in water, an increase of pH is observed from 5 to 8.9 and 10.1 using OST100 and OST950, respectively. In the presence of MB, the rise in pH is much more limited, up to 8.3 and 9.1. Thus, it can be proposed that the organic matter trapped in OST100 may contribute to the acid-base equilibrium and the MB sorption limits the protonated reactions and complex the negative charge of oxide OST surface. To analyze these data, it is very interesting to discuss the surface charge of adsorbent and MB dye. Quartz is the main component of OST shale that is negatively charged in used operatory conditions [21]. It is well admitted that the heat-treatment of OST increases the basicity of its surface such as conformed by pH measurements in the detriment on surface composition. Noticeably, the presence of organic matter in raw OST100 contributes to the acid-base properties of OST100 powder and its degradation at high temperature affects the material sorption properties. In addition, methylene blue has an aromatic amine groups with a pK_a of 3.8 and are mainly positively charged to pH 7. To clarify this point, the influence of pH on MB dye sorption at OST100 surface was studied. Using 20 ppm

Table 2
Langmuir and Freundlich constants for MB sorption on the OST100, OST550 and OST950 adsorbents

	Experimental q_{max} (±0.5 mg g^{-1})	Freundlich			Langmuir		
		K_f	$1/n$	R^2	$q_{e'L}$ (mg g^{-1})	(L mg^{-1})	R^2
OST100	>100	0.596	0.89	0.99295	333	0.44	0.7232
OST550	86	0.592	0.88	0.9925	200	0.46	0.7203
OST950	61	0.561	0.87	0.9967	111	0.45	0.8544

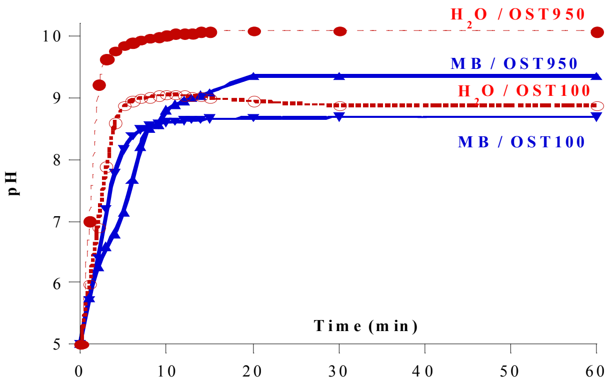

Fig. 6. Evolution of pH during the sorption process of MB on OST100 and OST950 adsorbents.

of MB as an initial concentration, a complete removal was obtained in pH 2–6 range, but decreased up the pH 7.

In addition, adsorption-regeneration tests were performed with OST550 sample. The choice of the temperature of calcination is related to the degradation of a major organic matter at this temperature as proved by thermogravimetric analysis. A first sorption of MB dye (20 mg L^{-1}) was performed and then the powder was treated to 550°C and the experiment re-conducted up to 3 times. The adsorption capacity of the once-regenerated OST550 sample (4.7 ± 0.2 mg · g^{-1}) was comparable to the pristine OST550 (4.9 ± 0.2 mg · g^{-1}). It was observed that there was no apparent change in adsorption capacity after regeneration up to 3 cycles while the average loss in photodegradation activity during regeneration was about 3–4% per cycle.

As comparison, the sorption capacities obtained in this work for MB sorption on Moroccan raw oil shale (>100 mg g^{-1}) and its thermal treated materials, OST550 (86 mg g^{-1}), OST950 (61 mg g^{-1}) are effective adsorbents compared to the other natural sorbents reported in the literature such as perlite (9 mg g^{-1}) [22], Abu-Tartour phosphate rock (100 mg g^{-1}) [23], Bengurir phosphate rock (22.5 mg g^{-1}) [7], natural zeolite (21 mg g^{-1}) [24]. This opens wide perspectives for these natural widely available low-cost resources as sorbents for the removal of other pollutants.

4. Conclusions

Overall, the oil shale has the advantage of a very low cost, low environmental impact and large abundance but exhibits a limited porosity. The MB sorption on dried and thermal treatment oil shale materials was carried out. Further, the adsorption process spontaneous follows pseudo-second order kinetics and the mechanism involved more than one process. The adsorption equilibrium data were fitted with the common adsorption isotherms as Freundlich equation was found to have the highest value of R^2 compared with other models. Experimental results showed that the surface adsorption was responsible for uptake of MB cationic dye on the oil shale.

Acknowledgments

This research was supported in part by the "Académie Hassan II des Sciences et Techniques". The authors thank Dr. T. Coradin and Dr. S. Masse (University of Pierre and Marie Curie - Paris France) for their scientific help and characterization of oil shale samples.

References

[1] V.K. Gupta, I. Ali, Removal of DDD and DDE from wastewater using bagasse fly ash, a sugar industry waste, Water Res., 35 (2001) 33.

[2] F. Gérard, Clay minerals, iron/aluminum oxides, and their contribution to phosphate sorption in soils, Geoderma, 262 (2016) 213–226.

[3] L. Clausen, I. Fabricius, L. Madsen, Adsorption of pesticides onto quartz, calcite, kaolinite, and alpha-alumina, J. Environ. Qual., 30 (2001) 846.

[4] F. Yang, S. Sun, X. Chen, Y. Chang, F. Zha, Z. Lei, Mg-Al layered double hydroxides modified clay adsorbents for efficient removal of Pb^{2+}, Cu^{2+} and Ni^{2+} from water, Appl. Clay Sci., 123 (2016) 134–140.

[5] S.C.R. Santos, R.A.R. Boaventura, Adsorption of cationic and anionic azo dyes on sepiolite clay: Equilibrium and kinetic studies in batch mode, J. Environ. Chem. Eng., 4 (2016) 1473–1483.

[6] Y. Hu, T. Guo, X. Ye, Q. Li, M. Guo, H. Liu, Z. Wu, Dye adsorption by resins: Effect of ionic strength on hydrophobic and electrostatic interactions, Chem. Eng. J., 228 (2013) 392–397.

[7] H. Bouyarmane, S. Saoiabi, A. Laghzizil, A. Saoiabi, A. Rami, M. El Karbane, Natural phosphate and its derivative porous hydroxyapatite for the removal of toxic organic chemicals, Desal. Water Treat., 52 (2014) 7265–7269.

[8] Z. Al-Qodah, A.T. Shawaqfeh, W.K. Lafi, Adsorption of pesticides from aqueous solutions using oil shale ash, Desalination, 208 (2007) 294–305.

[9] E. Tütem, R Apak, Ç.F Ünal, Adsorptive removal of chlorophenols from water by bituminous shale, Water Res., *32* (1998) 2315–2324.

[10] R. Shawabkeh, A. Al-Harahsheh, A. Al-Otoom, Copper and zinc sorption by treated oil shale ash. Sep. Pur. Technol., 40 (2004) 251–257.

[11] E.T. Acar, S. Ortaboy, G. Atun, Adsorptive removal of thiazine dyes from aqueous solutions by oil shale and its oil processing residues: Characterization, equilibrium, kinetics and modelling studies, Chem. Eng. J., 276 (2015) 340–348.

[12] A. Gouza, S. Saoiabi, S. Masse, A. Laghzizil, A. Saoiabi, Development and characterization of oil shale minerals for ciprofloxacin remediation, J. Chem. Pharm. Res., 6, (2014) 316–324.

[13] M. Elharti, K. Legrouri, E. Khouya, M. Oumam, H. Hannache, S. Fakhi, M. El Bouchti, N. Hanafi, B. Hammouti, Elimination of thorium ion by an adsorbent prepared from Moroccan oil shale of Timahdit activated by phosphoric acid, J. Chem. Pharm. Res., 4 (2012) 3460–3467.

[14] S. Ichchoa, E. Khouya, S. Fakhi, M. Ezzine, H. Hannache, R. Pallier, R. Naslain, influence of the experimental conditions on porosity and structure of adsorbents elaborated from Moroccan oil shale of Timahdit by chemical activation, J. Hazard. Mater., 118 (2005) 45–51.

[15] A. Singh, D.P. Dutta, J. Ramkumar, K. Bhattacharya, A.K. Tyagi, M.H. Fulekar, Serendipitous discovery of super adsorbent properties of sonochemically synthesized nano $BaWO_4$, RSC Adv., 3 (2013) 22580–22590.

[16] V. Srihari, A. Das, The kinetic and thermodynamic studies of phenol-sorption onto three agro-based carbons, Desalination, 225 (2008) 220–234.

[17] Y.S. Ho, Review of second-order models for adsorption systems, J. Hazard Mater., 136 (2006) 681–689.

[18] L.T. Zhuravlev, The surface chemistry of amorphous silica. Zhuravlev model, Colloids Surf. A., 17 (2000) 1–38.

[19] M. Zhao, Z. Tang, P. Li, Removal of methylene blue from aqueous solution with silica nano-sheets derived from vermiculite, J. Hazard. Mater., 158 (2008) 43.

[20] C.H. Weng, Y.F. Pan, Adsorption characteristics of methylene blue from aqueous solution by sludge ash, Colloids Surf. A., 274 (2006) 154–162.

[21] G.A. Parks, The isoelectric points of solid oxides, solid hydroxides, and aqueous hydroxocomplex systems, Chem. Rev., 65 (1965) 177–198.

[22] M. Dogan, M. Alkan, A. Türkyilmaz, Y. Özdemir, Kinetics and mechanism of removal of methylene blue by adsorption onto perlite, J. Hazard. Mater., B109 (2004) 141–148.

[23] G.F. Malash, M.I. El-Khaiary, Methylene blue adsorption by the waste of Abu-Tartour phosphate rock, J. Colloid Interf. Sci., 348 (2010) 537–545.

[24] R. Han, J. Zhang, P. Han, Y. Wang, Z. Zhao, M. Tang, Study of equilibrium, kinetic and thermodynamic parameters about methylene blue adsorption onto natural zeolite, Chem. Eng. J. 145 (2009) 496–504.

Appendix A.

N_2 sorption isotherms and BJH analysis and of the raw and heat-treated oil shale samples